

A Meter-Scale Plasma Wakefield Accelerator Driven by a Matched Electron Beam

P. Muggli,^{1*} B.E. Blue,² C.E. Clayton,² S. Deng,¹ F.-J. Decker,³ M.J. Hogan,³ C. Huang,²
R. Iverson,³ C. Joshi,² T.C. Katsouleas,¹ S. Lee,¹ W. Lu,² K.A. Marsh,² W.B. Mori,²
C.L. O'Connell,³ P. Raimondi,³ R. Siemann,³ and D. Walz³

¹*University of Southern California, Los Angeles, CA 90089, USA*

²*University of California, Los Angeles, CA 90095, USA*

³*Stanford Linear Accelerator Center, Stanford, CA 94309, USA*

(Received 13 December 2003)

A high-gradient, meter scale Plasma Wakefield Accelerator (PWFA) module operating in the nonlinear, electron blow-out regime is demonstrated experimentally. The beam and plasma parameters are chosen such that the matched beam channels through the plasma over more than twelve beta functions without spreading or oscillating over a range of densities for observing both deceleration and acceleration. The wakefield decelerates the bulk of the initially 28.5 GeV beam by up to 155 MeV, however particles in the back of the same beam are accelerated by up to 280 MeV at a density of $1.9 \times 10^{14} \text{ cm}^{-3}$ as the wakefield changes sign.

Work supported in part by the Department of Energy Contract DE-AC02-76SF00515
PACS: 41.75.Ht, 41.75.Lx, 52.40Mj

Plasma-based particle acceleration schemes [1] offer the possibility of accelerating charged particles to very high energies in a very short distance, and thereby significantly reducing the size and cost of a future particle accelerator for high-energy physics. These schemes use ultra-intense laser [2] or particle beams [3] as a source of free energy to excite the accelerating mode (a relativistic plasma wave or RPW) in a plasma. Gradients in excess of 100 GeV/m have been demonstrated using laser-driven RPWs [4-9], however, the acceleration length has been thus far limited to a few Rayleigh lengths (1-2 μm) because of the need to achieve high laser intensities by focusing the drive beam. Therefore, one of the key milestones in the realization of a high-energy plasma accelerator is increasing the length of the accelerator module to a meter-scale [1]. For a particle beam drivers, this needs to be achieved without significant transverse emittance growth. In this Letter, we present the first experimental demonstration of a meter-scale Plasma Wakefield Accelerator (PWFA) module, that is driven by an intense, ultra-relativistic (28.5 GeV) electron beam. The beam and plasma parameters are chosen such that the beam propagates through the plasma with a constant radius (i.e., matched) with minimal emittance growth at densities near the optimum for acceleration. At the optimum density for observing maximum acceleration [11], the electrons in the head of the beam drive a nonlinear plasma wakefield in the electron blowout regime [11-13]. The wakefield decelerates the bulk of the incoming 28.5 GeV beam by up to 155 MeV , however the particles in the back of the same beam are accelerated by up to 280 MeV as the wakefield changes sign. The accelerating gradient is roughly an order of magnitude larger than that in the 3 μm -long linac used to produce the drive beam. The results reported here therefore represent a first step toward a recently proposed concept to

increase the energy of a kilometers-long linear collider by adding much shorter, but ultra-high gradient plasma sections called afterburners [14].

Previous electron beam driven PWFA experiments have been performed with moderate incoming beam energies (of the order of 10 MeV) in ≈ 10 m long plasmas [15, 16] thereby limiting the possibility of energy gain to typically a few MeV. Recently a meter-scale PWFA module driven by a positron beam has also been demonstrated [17]. However, that experiment was performed in a lower charge regime with significantly smaller and linear wakefields.

Figure 1 shows the experimental set-up. The ultra-relativistic electron (e^-) beam from the Stanford Linear Accelerator is delivered to the Final Focus Test Beam line [18] with $N \approx 1.9 \times 10^{10}$ electrons per bunch at an energy, E , of 28.5 GeV and $\sigma_z \approx 700$ μ m (or $\sigma_z/c \approx 2.3$ ps). The incoming beam is focused near the entrance of the plasma, to a typical round spot size of $\sigma_{r0} \approx 30 \pm 2$ μ m. The beam has Gaussian profiles in the longitudinal and transverse dimensions, and σ_z and σ_r are the root mean square bunch length and spot radius respectively. The beam size before and after the plasma is monitored by imaging the optical transition radiation (OTR) emitted by single bunches when traversing ≈ 37 μ m thick titanium foils located approximately one meter upstream and downstream from the plasma [10, 19]. After exiting the plasma the beam travels through quadrupole and dipole (bending) magnets arranged in an imaging spectrometer configuration. The spectrometer has an effective energy resolution of ≈ 36 MeV for a beam size of 30 μ m at the plasma exit. The beam at the plasma entrance or at the plasma exit is imaged onto a 1 μ m thick piece of aerogel located 25 m downstream from the plasma, in the imaging plane of the magnetic spectrometer, where it emits Cherenkov radiation. The visible Cherenkov light

from the aerogel is imaged onto the slit of a streak camera to disperse in time the energy spectrum of the bunch. Time resolving the image of the beam at the plasma entrance in absence of plasma shows that the beam enters the plasma with a correlated energy spread (chirp) of $\approx 482 \text{ MeV}$, with the front of the bunch at higher energy than the back.

The plasma is created through single photon ionization of lithium vapor contained in a heat-pipe oven [20]. The plasma column is $\approx 1.4 \text{ m}$ long and has a typical transverse area of $\approx 0.12 \text{ m}^2$. The plasma density, n_e , is proportional to the energy of the ionizing ($\lambda = 193 \text{ nm}$) laser pulse, and can be varied between 0 and $\approx 2 \times 10^{14} \text{ m}^{-3}$. The value of n_e is calculated from laser energy absorption measurements and by fitting of an envelope model to the variations of the beam size observed as a function of the laser energy [21].

In the experiment reported here the beam charge density $n_b = N / (2\pi)^{3/2} \sigma_z \sigma_{r0}^2 \approx 2.8 \times 10^{15} \text{ m}^{-3}$ is much larger than the plasma density ($n_b > n_e$), the transverse beam size is smaller than the plasma collisionless skin depth ($\sigma_{r0} < c / \omega_p$; where $\omega_p = (n_e e^2 / \epsilon_0 m)^{1/2}$ is the electron plasma frequency), and the experiment is thus performed in the non-linear, blow out regime of the PWFA [11, 13]. In this regime, the particles in the head of the bunch expel all the plasma electrons from the bunch volume and create a pure ion column, which exerts a strong focusing force on the remainder of the bunch as it propagates through the plasma. The expelled plasma electrons rush back on the beam axis, behind the bunch, and create an electron density spike on the axis resulting in a highly nonlinear wakefield.

We have previously shown [21] that in this blow-out regime, the beam envelope dynamics are well described by an envelope model for the transverse beam size $\sigma_r(z)$: $\sigma_r(z)'' + K \sigma_r(z) - \epsilon^2 / \sigma_r(z)^3 = 0$. Here ϵ is the beam emittance and $K = e E_r / r m \omega_p^2 = \sigma_p^2 / (2\pi) c^2$ is the plasma focusing strength resulting from the radial field of the pure ion column:

$E_r = (en_e/2\epsilon_0)r$. A favorable situation is reached when the plasma and the beam are matched, which is achieved when the plasma focusing term K compensates for the beam divergence term arising from the finite beam emittance ϵ , i.e., when $K = \epsilon^2/\sigma_{r0}^4$. In this case, the beam focused at the plasma entrance ($\sigma_r(z=0)'=0$) propagates along the plasma with a constant transverse size σ_{r0} , i.e., the beam size at the plasma entrance.

In this experiment, the matching condition corresponds to a beam spot size of $33 \pm 3 \mu\text{m}$ for plasma densities in the range $1.2\text{--}2.5 \times 10^{14} \text{cm}^{-3}$. As shown in Fig. 2, the beam spot size recorded on the downstream OTR screen oscillates as the plasma density increases from low densities ($K < \epsilon^2/\sigma_{r0}^4$) toward the matched density ($K \approx \epsilon^2/\sigma_{r0}^4$). In this experiment the size of these oscillations decreases as the matching condition is approached, rather than increases as shown in Ref. 21 which was performed in the $K > \epsilon^2/\sigma_{r0}^4$ regime. Indeed, the beam size remains almost constant as the beam density is varied from $1.3\text{--}1.9 \times 10^{14} \text{cm}^{-3}$ indicating that the beam is close to being matched to the plasma. Imaging the beam at the plasma exit for $n_e > 7 \times 10^{13} \text{cm}^{-3}$ thus preserves the overall energy resolution of the spectrometer, and removes any contribution to the energy spectrum that could arise from a beam tail exiting the plasma with a transverse momentum [22].

The continuous curve shown on Fig. 2 is the result of the best fit of the envelope model to the experimental data and is a sensitive function of σ_{r0} , and ϵ , the beam parameters at the plasma entrance. In this experiment, the incoming beam beta function is $\beta_b = \sigma_{r0}^2/\epsilon = 0.11 \text{m}$. Therefore, Fig. 2 shows that at the highest densities, the matched beam is channeled over more than 12 beta functions, the beam beta function being the equivalent parameter to the Rayleigh length of a laser beam for a particle beam. Note that

an increase in beam emittance of 20% caused by the plasma would lead to a significant mismatch between the experimental data points and the envelope equation fit. Therefore the agreement between the fit and the data points on Fig. 2 shows that the plasma is “optically transparent” for the bulk of the beam and that the transverse emittance of the beam is preserved in this experiment.

In expelling the plasma electrons, the bunch electrons do work and therefore are expected to lose energy. However, as $2L_z$ approaches $\lambda_p/2 = \pi c/\omega_p$ (here for $n_e > 1.4 \times 10^{14} \text{ cm}^{-3}$, hereafter called the optimum density) the longitudinal component of the wakefield reverses sign within the bunch itself and can thus accelerate the electrons at the trailing end of the bunch. To observe this energy gain within single, chirped bunches the Cherenkov light was time resolved using an $\approx 1 \text{ ps}$ resolution streak camera. Single shot, streak camera images of the beam dispersed in energy and in time at a low ($n_e = 7 \times 10^{13} \text{ cm}^{-3}$) and a high ($n_e = 1.9 \times 10^{14} \text{ cm}^{-3}$) plasma density are shown in Fig. 3(a) and (b). At the low density, where the energy loss of the beam is small, the streak camera image is dominated by the incoming correlated energy spread on the beam. The crosses on these images mark the mean energy of the 1 ps wide slice at the beam center at these two densities. Comparison between these two images shows that at high n_e the center slice of the beam loses $\approx 170 \text{ MeV}$ energy, while the slices in the back of the beam gain energy.

To quantify the change in energy of the various slices of the beam, a set of streak camera data was taken as the plasma density was varied from below the optimum density for wakefield acceleration to near the optimum density. In Fig. 3(c) we show the energy of the individual 1 ps wide beam slices, after summing typically 10 individual streaks, at

three different plasma densities. For these three values of n_e the electron beam image size at the plasma exit (not shown) and therefore on the streak camera slit is almost constant. The red diamonds are for $n_e=7 \times 10^{13} \text{ cm}^{-3}$, and shows the front-to-back chirp seen in Fig. 3(a). This same chirp is also seen without the plasma, when imaging the beam at the plasma entrance location. As the density is increased to $1.6 \times 10^{14} \text{ cm}^{-3}$ (green squares) one can clearly see that nearly all the slices loose energy to various degrees relative to the low density data. At a density of $1.9 \times 10^{14} \text{ cm}^{-3}$, the energy loss for most of the slices is even greater, however, the last slice at +6 ps has in fact, gained energy. Figure 3(c) shows that at $n_e=1.9 \times 10^{14} \text{ cm}^{-3}$, the maximum beam energy loss is 230 MeV for the -1 ps slice and the energy gain is +85 MeV for the +6 ps slice.

Closer examination of Fig. 3(c) reveals that there is an apparent energy loss of ~ 50 MeV at $n_e=1.9 \times 10^{14} \text{ cm}^{-3}$ for a beam slice at -5 ps (beam front). This is however ≈ 5 times larger than that predicted by the linear theory for wakes induced by Gaussian beams [23] and than that found in fully nonlinear 3D, particle-in-cell simulations of the experiments [24]. These same simulations predict transverse focusing effects on the beam, which are in quantitative agreement with experimental observations. Therefore, it is reasonable to assume that the 50 MeV energy loss seen by the -5 ps slice at the head of the beam is due to a $\approx 40 \mu\text{m}$ vertical deflection of the whole beam at the exit of the $\approx 1.4 \text{ m}$ long plasma and that it is likely caused by the transverse density gradients in the plasma. We therefore assume that the slice at -5 ps at the front of the beam loses no energy for all shots at a given density. Now the energy variations induced by the PWFA interaction (see Fig. 4(a)) are obtained by first averaging all the streaks at a given density and then by subtracting slice-by-slice energies measured at the density of $n_e=7 \times 10^{13} \text{ cm}^{-3}$

(Fig. 3(c)) from the energies measured at higher densities to remove the time dependent incoming energy chirp. This procedure leaves a ± 45 MeV systematic experimental error bar on the energy change of individual slices.

At an average density of $1.5 \times 10^{14} \text{ cm}^{-3}$ (green squares, Fig. 4(a)), almost all slices of the bunch lose energy. The peak energy loss is 115 ± 45 MeV at $+1$ ps (relative to the bunch centroid). At this density the plasma wavelength of the nonlinear wake is too large to observe any significant energy gain. At a density of $1.9 \times 10^{14} \text{ cm}^{-3}$ (blue circles) the peak energy loss is larger, 155 ± 45 MeV, and occurs earlier in the bunch (-1 ps) because the plasma wavelength, which scales as $n_e^{-1/2}$, is shorter at this larger plasma density. Simultaneously, as expected now two later slices of the beam ($+5$ and $+6$ ps) gain energy with a maximum slice average energy gain of about 156 MeV observed for the $+6$ ps slice. The number of accelerated electrons in this 1 ps slice of the Gaussian beam is 3×10^7 .

The individual energy distributions of electrons in the last picosecond slices of Fig. 3 (see the vertical white lines at $+5.5$ ps) are examined further in Fig. 4(b). The distributions for the $n_e = 7 \times 10^{13} \text{ cm}^{-3}$ where energy gain is neither expected nor observed, and $n_e = 1.9 \times 10^{14} \text{ cm}^{-3}$ are shown (blue circles and red squares respectively). At $n_e = 1.9 \times 10^{14} \text{ cm}^{-3}$, the full width half maximum (FWHM) of this distribution is 280 MeV wider than the FWHM of the distribution for $n_e = 7 \times 10^{13} \text{ cm}^{-3}$. Therefore some electrons have gained at least 280 MeV energy at the higher density, consistent with approximately 290 MeV seen in 3D particle-in-cell code simulations of this experiment using the code OSIRIS [24, 25]. The peak gradient over the 1.4 cm long plasma is therefore 200 MeV/m. Thus the energy gain measurements corroborate the transverse spot size variation shown

in Fig. 2 in proving that the present experiment is indeed in the non-linear blowout regime of the PWFA. The detailed comparison between the experiment and the simulations will be published elsewhere.

Finally according to theory, the accelerating gradient in a PWFA scales approximately as N/σ_z^2 , the number of particles in the bunch divided by the square of the bunch length [12, 23]. Reducing of the bunch length by a factor of 10 is thus expected to bring the accelerating gradient in the 20 GeV/m range for the same beam charge at an appropriately optimized plasma density. Such large gradients are necessary to realize the recently proposed scheme to double the energy of a linear collider by placing few meter long, ultra-high gradient plasma sections just before the interaction point—A Plasma Afterburner [14].

This work is supported by the US DoE Grants No. DE-FG03-92ER40745, No. DE-AC03-76SF00515, No. DE-FG03-98DP00211, and No. DE-FG03-92ER40727, and No. DE-AC-03-76SF0098, and NSF grants No. ECS-9632735, No. DMS-9722121 and PHY-0078715. Dr. P. Tsou from JPL provided the aerogel.

e-mail address: muggli@usc.edu

- [1] T. Tajima and J. M. Dawson, *Phys. Rev. Lett.* **43**, 267 (1979).
- [2] C. Joshi *et al.*, *Nature* **311**, 525 (1984).
- [3] P. Chen *et al.*, *Phys. Rev. Lett.* **54**, 693 (1985).
- [4] D. Gordon *et al.*, *Phys. Rev. Lett.* **80**, 2133 (1998).
- [5] A. Modena *et al.*, *Nature* **377**, 606 (1995).
- [6] V. Malka *et al.*, *Science* **298**, 1596 (2002).
- [7] A. Ting *et al.*, *Phys. Rev. Lett.* **77**, 5377 (1996).
- [8] W. Leemans *et al.*, *Phys. Rev. Lett.* **89**, 174802 (2002).
- [9] D. Umstadter *et al.*, *Science* **273**, 472 (1996).
- [10] M. Hogan *et al.*, *Phys. Plasmas* **7**, 2241 (2000).
- [11] T. Katsouleas *et al.*, *Part. Accl.* **22**, 81 (1987).
- [12] C. Joshi *et al.*, *Phys. Plasmas* **9**, 1845 (2002).
- [13] J.B. Rosenzweig *et al.*, *Phys. Rev. A* **44**, R6189 (1991).
- [14] S. Lee *et al.*, *Phys. Rev. ST Accl. Beams* **5**, 011001 (2002).
- [15] N. Barov *et al.*, *Phys. Rev. ST Accl. Beams* **3**, 011301 (2000).
- [16] N. Barov *et al.*, *Phys. Rev. Lett.* **80**, 81 (1998).
- [17] B. Blue *et al.*, *Phys. Rev. Lett.* **90**, 214801 (2003).
- [18] V. Balakin *et al.*, *Phys. Rev. Lett.* **74**, 2479 (1995).
- [19] P. Catravas *et al.*, *Phys. Rev. E* **64**, 046502 (2001).
- [20] P. Muggli *et al.*, *IEEE Trans. on Plasma Sci.* **27** (3), 79 (1999).
- [21] C. E. Clayton *et al.*, *Phys. Rev. Lett.* **88**, 154801 (2002).

- [22] A. Geraci and D. H. Whittum, *Phys. Plasmas* **7**, 2241 (2000); B.E. Blue, Master Thesis, UCLA (2000).
- [23] W. Lu *et al.*, submitted to *Physics of Plasmas*.
- [24] S. Deng *et al.*, *AIP Conference Proceedings* 647, Ed. C. Clayton and P. Muggli, 592 (2002).
- [25] S. Lee *et al.*, *Phys. Rev. E* **61**(6), 7014 (2000).

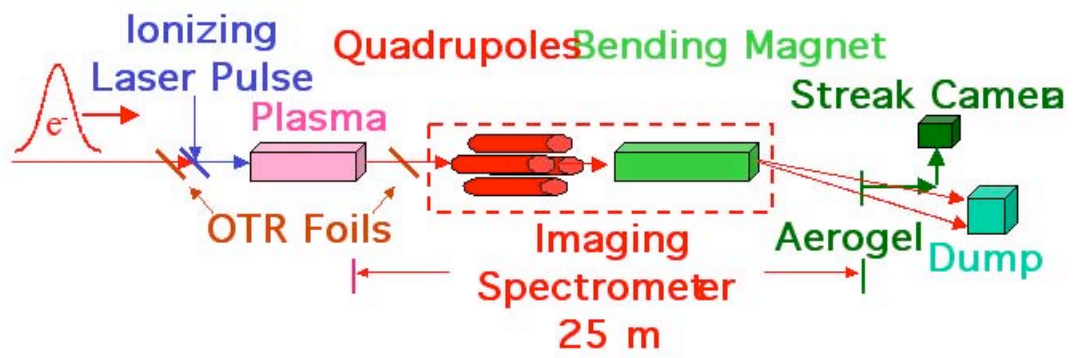


Figure 1

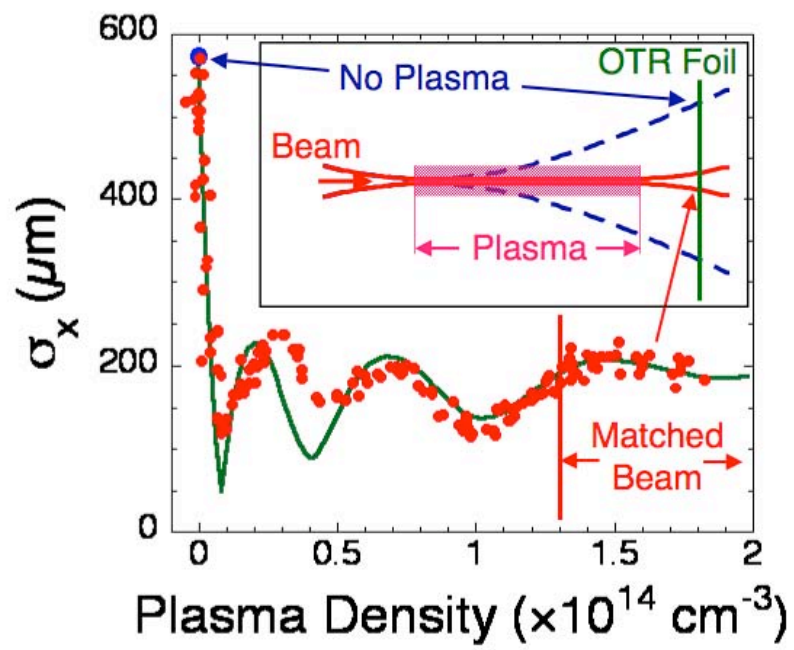


Figure 2

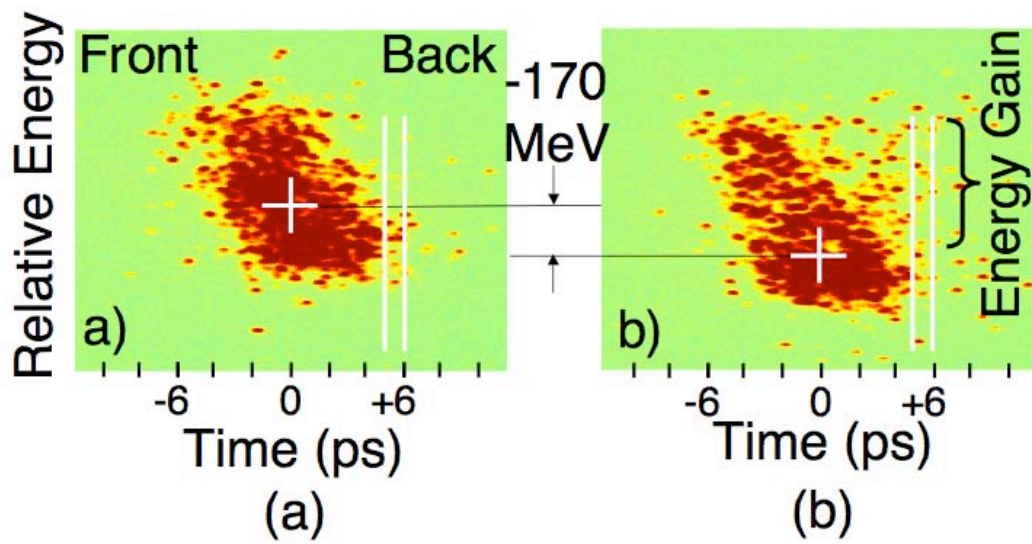


Figure 3 (a) and (b)

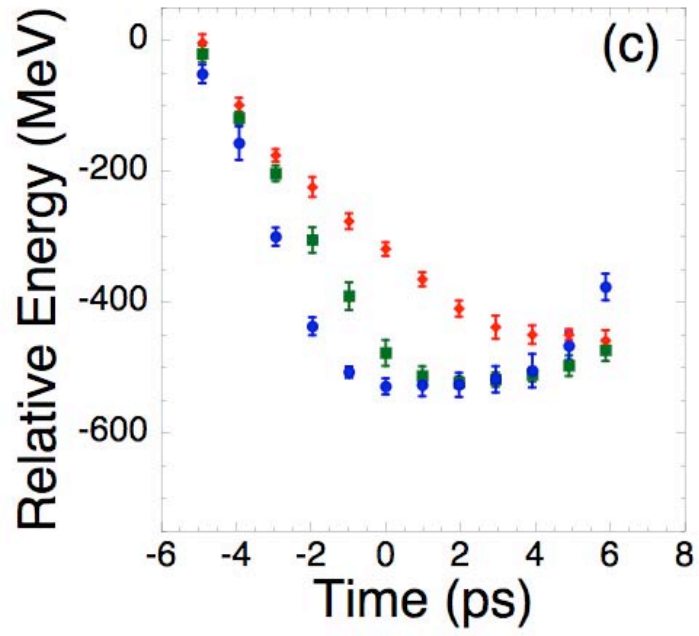


Figure 3(c)

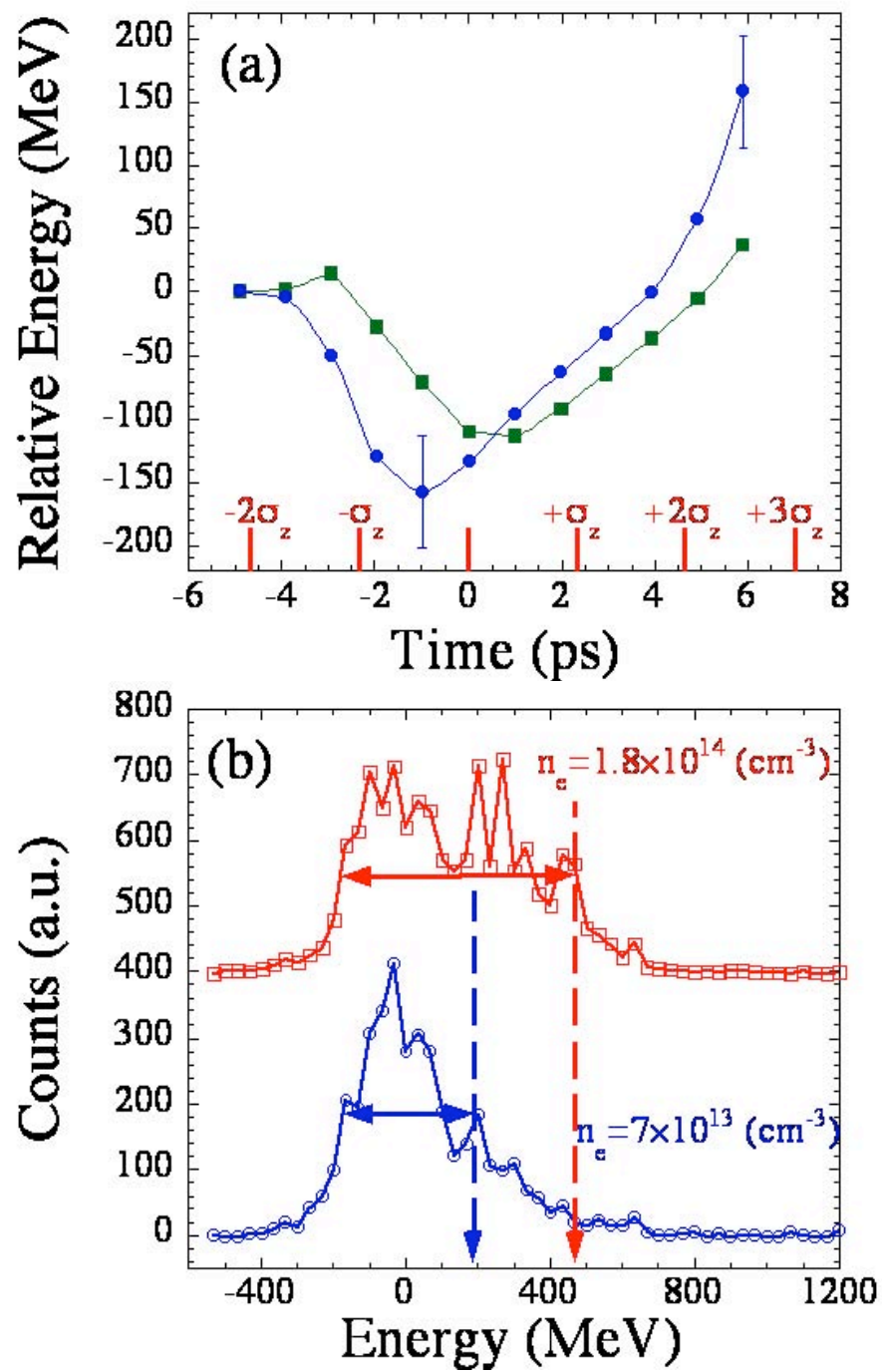


Figure 4

Figure captions

Figure 1: The schematic of the Plasma Wakefield Acceleration experimental set-up (not to scale).

Figure 2: The transverse size σ_x of the beam (red points) in the x-plane measured on the downstream OTR foil (see inset) as a function of plasma density. The green line is the best fit to the data using a beam envelope model in which $\sigma_{x0}=30\mu\text{m}$, $\sigma_k=8\times 10^{-9}\text{m-rad}$, and $\sigma_0=0.11\text{h}$.

Figure 3: Streak camera images of a single electron bunch dispersed in time and energy after propagation through (a) low density ($n_e=7\times 10^{13}\text{cm}^{-3}$), and (b) high density ($n_e=1.9\times 10^{14}\text{cm}^{-3}$) plasma (see text for details). The blue tick marks show the mean energy of picosecond wide slices of the beam. (c) Relative energy of the mean position of a picosecond wide slice of the beam vs. time calculated from the streak camera images for three different plasma densities: $n_e=7\times 10^{13}\text{cm}^{-3}$ (red diamonds), $1.6\times 10^{14}\text{cm}^{-3}$ (green squares), and $1.9\times 10^{14}\text{cm}^{-3}$ (blue circles), The curves are an average of ≈ 10 shots such as those shown in Fig. 3(a) and (b). The error bar (rms of the data) shows the vertical jitter in the data.

Figure 4: (a) Relative energy variations experienced by the mean of 1ps wide slices of the beam fitted with a Gaussian distribution at $n_e=1.5\times 10^{14}\text{cm}^{-3}$ (green squares), and $n_e=1.9\times 10^{14}\text{cm}^{-3}$ (red circles). These curves are obtained by averaging ≈ 10 individual streaks after lining up the first slice (-5ps) to remove any vertical pointing jitter of the

beam. (b) Relative energy distribution of the picosecond slice at +5.5 ps for $n_e=7 \times 10^{13} \text{ cm}^{-3}$ (blue curve) and $n_e=1.9 \times 10^{14} \text{ cm}^{-3}$ (red curve, shifted vertically). The horizontal arrows are the full widths at half maximum of the distributions.